WORLD JOURNAL OF PHARMACEUTICAL RESEARCH
Coden USA: WJPRAP Impact Factor 8.63
Volume 15, Issue 8, 436-456. Research Article ISSN 2277–7105

COMPUTATIONAL DESIGN AND MOLECULAR DOCKING OF PYRAZOLONE DERIVATIVES DERIVED FROM IMIDAZOLE HYDRAZIDE AGAINST SARS-COV-2 MAIN PROTEASE

Anjana V. S.*, Rose Mary Joseph, Ajna S. A., Anchu Raj, Chandu Nath

Department of Pharmaceutical Chemistry; Mar Dioscorus College of Pharmacy Alathara, Thiruvanathapuram.

Article Received on 15 March 2026,
Article Revised on 04 March 2026,
Article Published on 16 April 2026,

https://doi.org/10.5281/zenodo.19591863

***Corresponding Author**

Anjana V. S.
Department of Pharmaceutical Chemistry; Mar Dioscorus College of Pharmacy Alathara, Thiruvanathapuram.

How to cite this Article: Anjana V. S.*, Rose Mary Joseph, Ajna S. A., Anchu Raj, Chandu Nath (2026). Computational Design And Molecular Docking Of Pyrazolone Derivatives Derived From Imidazole Hydrazide Against Sars-Cov-2 Main Protease. World Journal of Pharmaceutical Research, 15(8), 436–456.

ABSTRACT

The emergence of SARS-CoV-2 has highlighted the urgent need for effective antiviral agents, prompting the exploration of novel heterocyclic scaffolds through computational drug design approaches. In the present study, a series of fifty novel pyrazolone derivatives derived from imidazole hydrazide were designed and evaluated as potential inhibitors of the SARS-CoV-2 main protease (Mpro, PDB ID: 6LU7). The chemical structures of the compounds were drawn and optimized using ACD/ChemSketch software. The designed compounds were further assessed for drug-likeness through Lipinski's rule of five using Molinspiration software, where all derivatives showed acceptable physicochemical properties. Biological activity prediction was carried out using PASS software, indicating favorable probabilities for antiviral activity. ADMET profiling further supported the suitability of the compounds for oral administration. Molecular docking studies were performed using AutoDock against SARS-CoV-2 Mpro, and several derivatives exhibited binding affinities comparable to or better than the standard drug ritonavir. Among them, compound A49 demonstrated the most promising docking score, suggesting strong interaction with the active site of the target enzyme. Overall, the study identifies pyrazolone–imidazole hydrazide derivatives as promising lead candidates for further synthesis and experimental validation as potential anti-COVID-19 agents.

KEYWORDS: Pyrazolone derivatives, SARS-CoV-2, Main protease (Mpro), Molecular docking, In silico drug design, AutoDock.

1. INTRODUCTION

Chemistry has played an integral part in drug discovery and development and will continue to be essential in addressing the global health challenges we face as a society.[1] Medicate revelation is troublesome, perilous, costly and time-consuming. It more often than not takes 10 to 15 a long time for a medicate to come to advertise. Luckily, we can speed up this prepare with the offer assistance of computational chemistry and computational sedate disclosure. Since computational strategies are anvital portion of intrigue pharmaceutical investigate, it is critical to get it the instruments utilized and their openings and impediments. The best medicate revelation unit combines the logical information of a few areas, such as science, chemistry, and clinical science.[2]

1.2 DRUG DESIGN

Drug design may be defined as an effort to develop a new drug by molecular modification of lead compound for optimization of desired effects and minimization of side effects. Drug design is the approach of finding drugs by design, based on their biological targets.

Two major types of drug design.

1. Ligand based drug design (indirect drug design)
2. Structure based drug design (direct drug design)

Coronaviruses are a large family and a subset of Nido viral order, Coronaviridae family, Coronavirinae subfamily. These viruses can cause a disease ranging from the common cold to more severe respiratory diseases and respiratory distress or acute respiratory distress syndrome (ARDS. Severe acute respiratory syndrome coronavirus 2 (SARS-CoV-2) is a novel coronavirus that has caused a pandemic of acute respiratory syndrome in humans following the outbreaks of Severe Acute Respiratory Syndrome Coronavirus (SARS-CoV) and Middle East Respiratory Syndrome Coronavirus. Since the outbreak of COVID-19, over 600 million people have been confirmed to have tested positive for the virus, and more than 6 million patients have died. SARS-CoV-2 shares all typical structural features of other coronaviruses. However, compared with SARS CoV, SARS-CoV-2 has certain structural changes that render it more infectious. Similar to SARS-CoV, SARS-CoV-2 enters the cells by binding to its primary functional receptor, angiotensin-converting enzyme 2 which is

widely distributed in epithelial cells and in endothelial cells of tissues and organs throughout the body.[3]

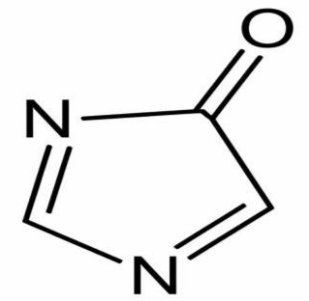

Fig 1: Structure of Pyrazolone.

Pyrazolones are five-membered heterocyclic compounds containing one ketonic group and two adjacent nitrogen atoms. The principal reactive centres within the pyrazolone nucleus include the nucleophilic nitrogen atoms (N1 and N2), the electrophilic carbonyl carbon at the C3 position, and the active methylene or methine carbon at C4. These reactive sites enable a wide range of chemical transformations, including mono- and di substitution at the C4 position, fused ring cyclization, and 1,2-nitrogen-based hetero-cyclization, thereby facilitating the synthesis of structurally diverse derivatives with controlled stereochemistry and enhanced biological activity.[5]

1.3 SCHEME OF WORK

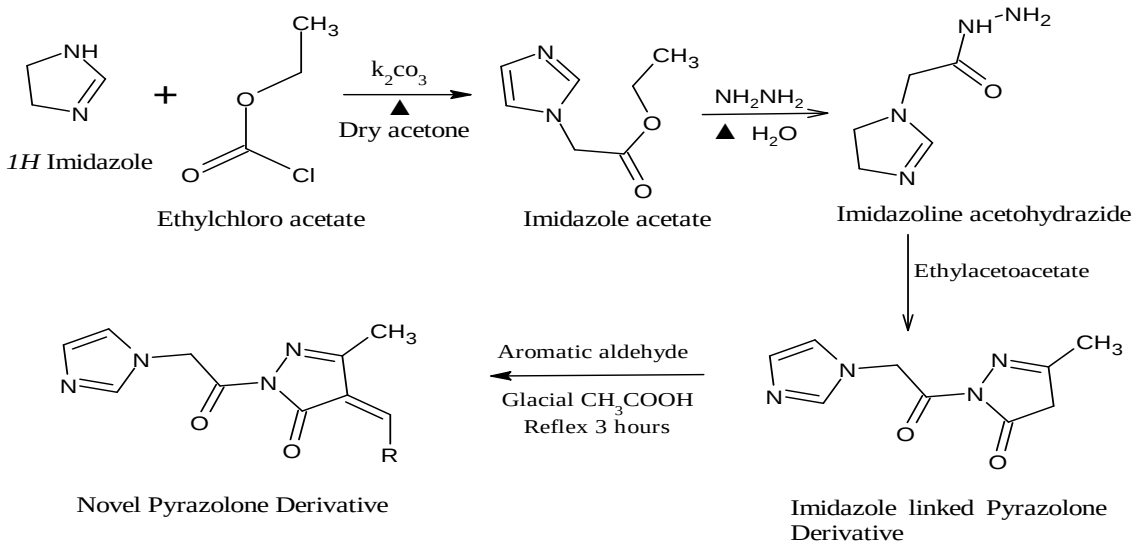

2. OBJECTIVES OF STUDY

COVID-19, caused by SARS-CoV-2, remains a global health concern due to its rapid transmission and potential severity. The main protease (Mpro) of SARS-CoV-2 plays a

crucial role in viral replication and transcription, making it an attractive therapeutic target. Although several antiviral agents have been explored, the need for safer and more effective inhibitors persists. Pyrazolone derivatives are known for their diverse pharmacological activities, including antiviral and anti-inflammatory properties. Studies suggest that structural modification of bioactive scaffolds can enhance inhibitory activity and reduce toxicity. Therefore, an attempt is made to design and evaluate novel pyrazolone analogues derived from imidazole hydrazide to investigate their inhibitory potential against the SARS-CoV-2 main protease.So the main objective of the present work involves design of Pyrazolone derivative derived from Imidazole Hydrazide and exploring their anti-viral activity.

***Insilico* screening**

I. Design of novel compounds and conduct of Lipinski analysis

Based on the literature review, it was concluded that Pyrazolone derived Imidazole Hydrazide compounds exhibit activity against COVID 19. Novel derivatives of Pyrazolone derived Imdazole Hydrazide are intended to be designed by utilizing ACD Lab Chemsketch 12.0 Software.

II. Molinspiration

All developed leads will undergo Lipinski rule analysis using Molinspiration Software to identify biologically active compounds that adhere to “Lipinski’s rule of five” and demonstrate drug likeness.

III. PASS (Prediction of Activity Spectra for Substances)

It is widely recognized as the leading tool for determining sample sizes in various fields such as clinical trials, pharmaceuticals, and medical research. Inputting the structural formula of a drug-like substance into specialized software can provide an estimated biological activity profile as an output.

IV. ADMETlab (Absorption, Distribution, Metabolism, Excretion, and Toxicity Laboratory)

ADMETlab is a widely used computational tool in drug discovery that predicts the pharmacokinetic and toxicity profiles of chemical compounds based on their molecular structure. By inputting the structure of a drug-like molecule into the software, it provides detailed insights into absorption, distribution, metabolism, excretion, and toxicity properties, helping researchers evaluate the safety and efficacy of compounds at an early stage.

V. Docking studies

The proposed compounds will undergo docking studies using Autodock4 against the selected target protein (pdb: 6LU7) aiming to assess their potential antiviral activity. Based on the docking results, the compounds show highest docking score will be chosen for further studies.

3. MATERIALS AND METHODS

3.1 *Insilico* screening

The proposed structure of novel Pyrazolone derivatives derived from Imidazole Hydrazide underwent *insilico* screening using a range of computational chemistry software tools including ACD Lab/ Chem Sketch 12.0, Molinspiration , PASS,ADMET and Auto Dock Vina.

3.1.1 ACD/Chemsketch

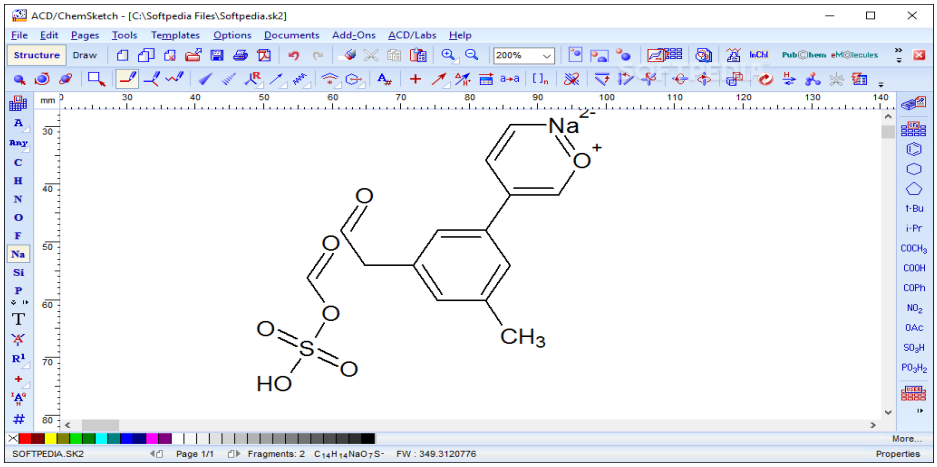

Figure 2: Chemsketch Window.

ACD/Chem Sketch Freeware is a versatile drawing package enabling users tocreate chemical structures encompassing organics, organometallics, polymers, and Markush structures. It offers features like calculation of molecular properties (e.g., molecular weight, density, molar refractivity etc.), 2D and 3D structure cleaning and viewing, naming structures (fewer than 50 atoms and 3 rings), and predicting log P values. ACD/ Chemsketch offers the following major capabilities.[6]

3.1.2 Molinspiration

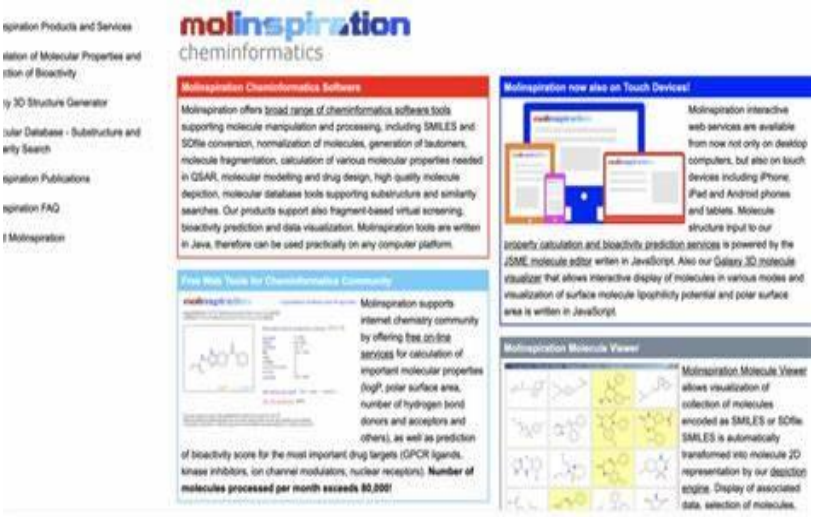

Fig 3: Molinspiration window.

"Molinspiration" specialises in utilizing model cheminformatic techniques, with a particular emphasis on internet -based application, to enhance drug discovery and molecular design process. It provides a comprehensive suite of cheminformatics software tools. These tools support a wide range of functions, SMILES and SD file conversion, normalizing molecules, generating tautomers, molecule fragmentation, calculating various molecular properties essential for QSAR (Quantitative Structure-Activity Relationship) studies, molecular modelling and drug design, high-quality molecule depiction, molecular database tools supporting substructure search or similarity and pharmacophore similarity search. The designed compound undergoes Lipinski rule analysis using Molinspiration software to identify potentially biologically active compounds. Lipinski rule, also known as Pfizer's rule five or Lipinski's rule of five, was formulated by the scientist Christopher A Lipinski.

The Lipinski's rule of five states that an orally active drug should obey the following criteria:

1. Not more than five hydrogen bond donors.
2. Not more than 10 hydrogen bond acceptors.
3. Molecular weight less than 500 Daltons.
4. An octanol-water partition coefficient log P not greater than 5
5. Not more than 5 rotatable.[7]

3.1.3 PASS (Prediction of Activity Spectra for Substances)

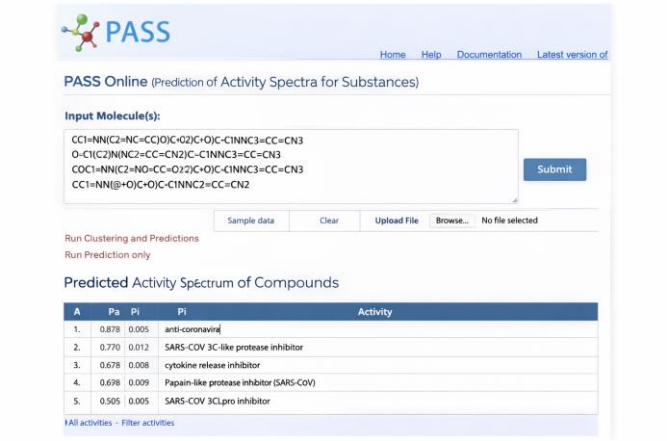

Fig 4: Pass online.

PASS is a program used for calculating sample sizes or determining the statistical power of a test or confidence interval in research studies. NCSS LLC is the company that produces PASS. It is a comprehensive software package with over 290 documented sample size and power procedures. It's widely recognized as the leading tool for determining sample sizes in various fields such as clinical trials, pharmaceuticals, and medical research. Inputting the structural formula of a drug-like substance into specialized software can provide an estimated biological activity profile as an output.

4.1.4 ADMET lab 3.0

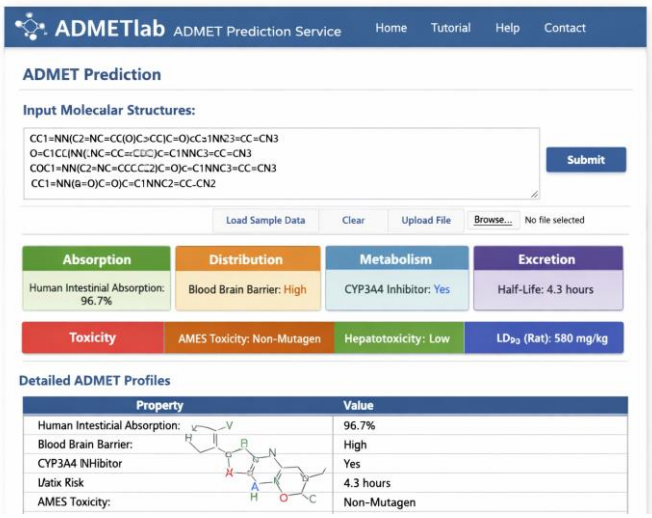

Fig 5: ADMET lab.

It provides a comprehensive and efficient platform for evaluating ADMET-related parameters as well as physicochemical properties and medicinal chemistry characteristics involved in the

drug discovery process.

3.1.4 Protein Data Bank

The Protein Data Bank (PDB) is a online database that stores three-dimensional structural data of large biological molecules, including proteins and nucleic acid. This data is gathered using techniques like X-ray crystallography, NMR spectroscopy, and cryo-electron microscopy. Scientists worldwide contribute to the database, and the information is freely accessible through member organization websites like PDBe, PDBj, RCSB and BMRB. The Protein Data Bank (PDB)is overseen by the Worldwide Protein Bank(wwPDB), an organization responsible for managing and maintaining the database. The PDB plays a crucial role in structural biology, particularly in areas like structural genomics. Many top scientific journals and funding agencies now mandate scientists to submit their structural data to the Protein Data Bank (PDB).[8,9,10]

3.1.5 Protein preparation

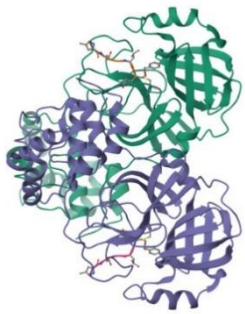

Figure 6:3D Structure of SARS COV 2 Main Protease.

The typical structure file from the PDB may require preprocessing before it can be readily utilized in molecular modelling calculations. It consists of only heavy atoms and may include a co-crystallized ligand, water molecules, metal ions, activators, cofactors and several protein subunits. According to the requirement protein is pre-processed, optimized and minimized with forcefield. Optimization involves water removal and minimization. The protein structure was refined. The ionization structure and most stable were chosen.

3.1.6 Ligand preparation

Ligand preparation involved energy of the ligands. Ligprep [Schrodinger, 2010] facilitated this process by adding hydrogen, converting 2D structures to 3D, generating stereoisomers, and optionally neutralizing charged structures or determining the most probable ionization

state at a user-defined PH. All the structures were ionized at a neutral pH of 7. Conformers for each ligand were generated using Conf Gen, applying the OPLS-2005 force field method.[11,12,13]

3.1.7 DOCKING

Molecular docking is a computational technique used to predict the preferred orientation and structure of an intermolecular complex formed between two molecules. Typically, a small molecule known as the ligand interacts with specific regions of a target protein called binding sites, which are responsible for biological activity and ligand recognition. Docking studies generate multiple possible conformations, referred to as binding modes, and evaluate the stability of the resulting complexes. The method estimates binding affinity by calculating interaction energies using scoring functions, which help identify the most favorable ligand–protein interaction.

The docking process generally involves two main steps: conformational sampling and scoring. During conformational sampling, various orientations and positions of the ligand within the active site are explored. In the scoring phase, each pose is evaluated based on parameters such as hydrogen bonding, hydrophobic interactions, van der Waals forces, and electrostatic interactions. Advanced docking algorithms may also account for ligand flexibility and, in some cases, limited protein flexibility to better mimic biological conditions.

Molecular docking plays a crucial role in structure-based drug design by helping researchers identify potential lead compounds, understand molecular mechanisms of binding, and optimize pharmacological activity. It reduces the need for extensive experimental screening, thereby saving time and cost in drug discovery. Furthermore, docking studies can provide insights into structure–activity relationships (SAR) and guide rational modification of chemical structures to enhance potency and selectivity.

3.1.7 AutoDock

AutoDock comprises 3 C programs, AutoTors, responsible for refining ligand input, AutoGrid, which calculates interaction energies using macromolecular coordinates, and AutoDock itself, tasked with the actual docking process. AutoDock effectively reproduces ligand positions by considering six spatial degrees of freedom-rotation and translation. It accurately captures crystallographically determined positions for ligands with up to eight torsional degrees of freedom. It’s simulated annealing search may struggle to adequately explore conformational

space for molecules with a high number of degrees of freedom, potentially limiting its applicability in certain cases.[14,15]

SERIAL NUMBER	COMPOUND CODE	FUCNCTIONAL GROUP
1.	a1	C_6H_6
2.	a2	$C_6H_5OCH_3$
3.	a3	$C_6H_5OC_2H_5$
4.	a4	C_6H_5F
5.	a5	C_6H_5F
6.	a6	C_6H_5F
7.	a7	$C_6H_5OCH_3$
8.	a8	C_6H_5Cl
9.	a9	C_6H_5Cl
10.	a10	C_6H_5Br
11.	a11	C_6H_5Br
12.	a12	C_6H_5Br
13.	a13	C_6H_5Cl
14.	a14	$C_6H_5CH_3$
15.	a15	$C_6H_5OCH_3$
16.	a16	$C_6H_5OCH_3$
17.	a17	$C_6H_5OCH_3$
18.	a18	$C_6H_5OC_2H_5$
19.	a19	$C_6H_5OC_2H_5$
20.	a20	$C_6H_5OC_2H_5$
21.	a21	$C_6H_5OC_2H_5$
22.	a22	$C_6H_5NH_2$
23.	a23	$C_6H_5NH_2$
24.	a24	$C_6H_5NH_2$
25.	a25	$C_6H_5NO_2$
26.	a26	$C_6H_5NO_2$
27.	a27	$C_6H_5NO_2$
28.	a28	C_6H_5OH
29.	a29	C_6H_5OH
30.	a30	C_6H_5OH
31.	a31	$C_6H_5OH_2$
32.	a32	$C_6H_5OH_2$
33.	a33	$C_6H_5(NH_2)_2$
34.	a34	$C_6H_5Cl_3$
35.	a35	$C_6H_5Cl_3$
36.	a36	$C_6H_5Cl_2$
37.	a37	$C_6H_5Cl_2$
38.	a38	$C_6H_5Cl_2$
39.	a39	$C_6H_5Cl_2$
40.	a40	$C_6H_5F_2$
41.	a41	$C_6H_5F_2$
42.	a42	$C_6H_5F_2$

43.	a43	$C_6H_5Br_2$
44.	a44	$C_6H_5Br_2$
45.	a45	$C_6H_5Br_2$
46.	a46	$C_6H_5Br_2$
47.	a47	$C_6H_5F_2$
48.	a48	$C_6H_5Cl_2$
49.	a49	$C_6H_5OH_2$
50.	a50	$C_6H_5(CH_3)_2$

4. RESULT AND DISCUSSION

Fifty analogues of Pyrazolone derivatives were designed using ACD Lab Chemsketch 12.0. Initially the designed fifty analogues were subjected to Lipinski rule analysis using molinspiration software.

4.1Theoretical determination of drug-likeness properties

We predicted the drug likeliness profile of the compounds through analysis of pharmacokinetic properties of the compounds by using molinspiration online software. Based on the results obtained from molinspiration it was observed that all of the proposed compounds obeyed Lipinski rule of five. According to the Lipinski's rule of five new molecule designed for oral route should have a MW < 500, log P o/w < 5, No more than 5 hydrogen bond donors and No more than 10 hydrogen bond acceptor. From the Lipinski rule analysis, all the 50 compounds were selected for further studies, since the compound did not show any violations from the Lipinski rule of five. Structure of proposed pyrazolone derivative of Imidazole Hydrazide.

The results of Lipinski rule analysis of first 50 compounds are shown in the table 1.

Table 1: Lipinski Rule Analysis of Proposed Derivatives.

Sl.no	Compound Code	Molecular weight <500	No. of hydrogen bond donors <5	No. of hydrogen bond acceptors <10	Log p value <5	No. of Rotatable bond <10	No. of violation
1.	a1	296.33	0	6	1.20	3	0
2.	a2	338.37	0	7	1.08	4	0
3.	a3	352.39	0	7	1.58	5	0
4.	a4	314.32	0	6	1.32	3	0
5.	a5	314.32	0	6	1.37	3	0
6.	a6	314.32	0	6	1.34	3	0
7.	a7	310.36	0	6	1.63	3	0
8.	a8	330.77	0	6	1.83	3	0

9.	a9	330.77	0	6	1.88	3	0
10.	a10	375.23	0	6	1.96	3	0
11.	a11	375.23	0	6	2.01	3	0
12.	a12	375.23	0	6	1.99	3	0
13.	a13	330.77	0	6	1.86	3	0
14.	a14	310.36	0	6	1.60	3	0
15.	a15	310.36	0	6	1.63	3	0
16.	a16	338.37	0	7	1.05	4	0
17.	a17	338.37	0	7	1.10	4	0
18.	a18	338.37	0	7	1.08	4	0
19.	a19	352.39	0	7	1.56	5	0
20.	a20	352.39	0	7	1.60	5	0
21.	a21	352.39	0	7	1.58	5	0
22.	a22	311.35	2	7	0.64	3	0
23.	a23	311.35	2	7	0.28	3	0
24.	a24	311.35	2	7	0.25	3	0
25.	a25	341.33	0	9	1.11	4	0
26.	a26	341.33	0	9	1.16	4	0
27.	a27	341.33	0	9	1.14	4	0
28.	a28	312.33	1	7	1.14	3	0
29.	a29	312.33	1	7	0.70	3	0
30.	a30	312.33	1	7	0.72	3	0
31.	a31	328.33	2	8	0.23	3	0
32.	a32	328.33	2	8	0.64	3	0
33.	a33	326.36	4	8	-0.31	3	0
34.	a34	326.36	4	8	0.10	3	0
35.	a35	399.67	0	6	3.09	3	0
36.	a36	365.22	0	6	2.46	3	0
37.	a37	365.22	0	6	2.49	3	0
38.	a38	365.22	0	6	2.49	3	0
39.	a39	365.22	0	6	2.419	3	0
40.	a40	332.31	0	6	1.46	3	0
41.	a41	332.31	0	6	1.46	3	0
42.	a42	332.31	0	6	1.46	3	0
43.	a43	454.12	0	6	2.75	3	0
44.	a44	454.12	0	6	2.75	3	0
45.	a45	454.12	0	6	2.75	3	0
46.	a46	454.12	0	6	2.73	3	0
47.	a47	332.31	0	6	1.46	3	0
48.	a48	365.22	0	6	2.49	3	0
49.	a49	328.33	2	8	0.23	3	0
50.	a50	324.38	0	6	2.03	3	0

The results of Lipinski rule analysis of first 50 compounds are shown in the table 1. The designed fifty analogues were subjected to Lipinsky rule analysis using molinspiration software. From the results of Lipinski rule analysis, all the 50 compounds were selected for further studies, since the compounds did not show any violation from the Lipinsky rule of

five. From the results of Lipinski rule analysis, all the 50 compounds were selected for further studies, since the compounds did not show any violation from the Lipinsky rule of five. The drug-likeness of the designed compounds (a1–a50) was evaluated based on Lipinski's Rule of Five, which predicts oral bioavailability. All compounds showed zero violations, indicating full compliance with the rule. The molecular weight of the compounds ranged from 296.33 to 454.12 Da, remaining within the acceptable limit of less than 500 Da. The number of hydrogen bond donors (0–4) and hydrogen bond acceptors (6–9) were also within permissible limits, supporting favorable interaction potential with biological targets. The Log P values ranged from -0.31 to 3.09, suggesting balanced lipophilicity, which is essential for membrane permeability and solubility. Additionally, all compounds possessed fewer than 10 rotatable bonds, indicating suitable molecular flexibility. Some compounds such as a33 and a34 showed lower Log P values indicating higher hydrophilicity, whereas compounds like a35 and a43–a46 exhibited relatively higher lipophilicity, yet remained within acceptable limits. Overall, the absence of Lipinski violations confirms that all compounds possess favorable physicochemical properties and are likely to exhibit good oral bioavailability, making them promising candidates for further drug development studies.

4.2 PASS (Prediction of Activity Spectra for probability to be active and Pi indicates probability Substances to be inactive)

The PASS value of proposed derivatives were shown in table 2. The PASS software predicts the biological activity of proposed derivatives where Pa indicates probability to be active and pi indicate probability to be inactive.

Table 2: PASS of designed 50 compounds.

COMPOUND CODE	Pa	Pi
a1	0232	0072
a2	0242	0065
a3	0252	0059
a4	0208	0089
a5	0208	0089
a6	0198	0097
a7	0231	0072
a8	0173	0129
a9	0203	0093
a10	0221	0079
a11	0216	0083
a12	0214	0084
a13	0173	0129

a14	0188	0108
a15	0236	0069
a16	0217	0082
a17	0238	0067
a18	0238	0067
a19	0230	0073
a20	0248	0061
a21	0252	0059
a22	0222	0078
a23	0245	0063
a24	0249	0060
a25	0259	0127
a26	0277	0147
a27	0187	0109
a28	0273	0047
a29	0236	0069
a30	0239	0067
a31	0260	0054
a32	0268	0050
a33	0220	0080
a34	0230	0073
a35	0155	0079
a36	0157	0081
a37	0159	0149
a38	0194	0101
a39	0193	0102
a40	0176	0125
a41	0202	0094
a42	0197	0099
a43	0209	0088
a44	0201	0095
a45	0202	0093
a46	0181	0119
a47	0201	0029
a48	0177	0123
a49	0194	0101
a50	0241	0065

All the fifty analogues of Pyrazolone derived Imidazole Hydrazide were shown antiviral activity against SARS COV 2 Main Protease. The PASS prediction results of the designed compounds (a1–a36) were compared with a standard drug to evaluate their potential biological activity. Typically, standard drugs exhibit higher Pa values (generally >0.5) with significantly lower Pi values, indicating strong and well-established biological activity. In contrast, the synthesized compounds showed moderate Pa values ranging from 0.155 to 0.277, with all compounds maintaining Pa > Pi, suggesting a favorable probability of activity.

Among the series, compounds such as a26, a28, a31, and a32 demonstrated relatively higher Pa values, approaching the activity trend of the standard drug, although still lower in magnitude. Notably, a28 exhibited a good balance of higher Pa and lower Pi, indicating better predictive reliability. While none of the compounds reached the activity level of the standard drug, their consistent Pa > Pi profile suggests that they possess promising biological potential.

Overall, although the activity prediction of the designed compounds is lower than that of the standard drug, their moderate PASS scores indicate that they can serve as lead molecules for further optimization and experimental validation.

4.3 ADMETlab 3.0

ADMETlab 3.0 is used for predicting absorption, distribution, metabolism, excretion, and toxicity (ADMET) properties of chemical compounds. MDCK permeability inhibitor, CYPA12 inhibitor, Volume of distribution, CYP209, Plasma clearance, half-life, Drug induced liver toxicity, Carcinogenicity of 50 analogue were determined by ADMET LAB 3.0.

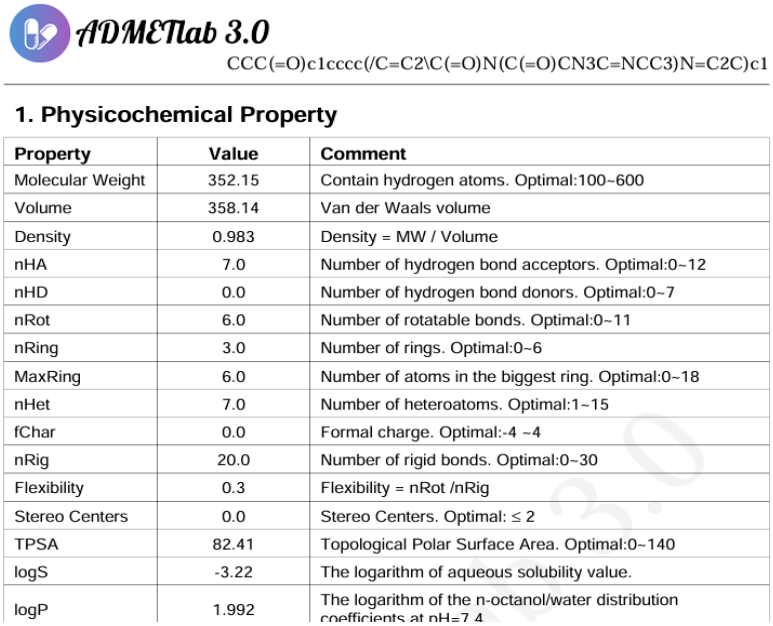
ADMETlab 3.0

CCC(=O)c1cccc(/C=C2\C(=O)N(C(=O)CN3C=NCC3)N=C2C)c1

1. Physicochemical Property

Property	Value	Comment
Molecular Weight	352.15	Contain hydrogen atoms. Optimal:100~600
Volume	358.14	Van der Waals volume
Density	0.983	Density = MW / Volume
nHA	7.0	Number of hydrogen bond acceptors. Optimal:0~12
nHD	0.0	Number of hydrogen bond donors. Optimal:0~7
nRot	6.0	Number of rotatable bonds. Optimal:0~11
nRing	3.0	Number of rings. Optimal:0~6
MaxRing	6.0	Number of atoms in the biggest ring. Optimal:0~18
nHet	7.0	Number of heteroatoms. Optimal:1~15
fChar	0.0	Formal charge. Optimal:-4 ~4
nRig	20.0	Number of rigid bonds. Optimal:0~30
Flexibility	0.3	Flexibility = nRot /nRig
Stereo Centers	0.0	Stereo Centers. Optimal: ≤ 2
TPSA	82.41	Topological Polar Surface Area. Optimal:0~140
logS	-3.22	The logarithm of aqueous solubility value.
logP	1.992	The logarithm of the n-octanol/water distribution coefficients at pH=7.4

Fig 6: ADMET.

Table 3: ADMET Analysis.

COMPOUND CODES	ABSORPTION			DISTRIBUTION	METABOLISM		EXCRETION		TOXICITY	
	MDCK PERMEABILITY	PGP INHIBITOR	CYP1A12	VDSS	CYP1A2	CYP209	CL PLASMA	T1/2	DILI	CARCINOGENICITY
a1	-4.724	0.745	0.305	0.004	0.977	0.0804	4.264	1.204	0.905	0.868
a2	-0.637	0.604	4.961	0.018	0.036	0.05	5.586	0.922	0.926	0.889
a3	4.884	0.378	0.58	0.121	0.121	0.005	6.359	0.7582	0.851	0.881
a4	-4.724	0.745	0.305	0.004	0.977	0.804	4.264	1.204	0.868	0.905
a5	-4.724	0.745	0.305	0.004	0.977	0.804	4.264	1.204	0.905	0.868
a6	-4.672	0.574	0.932	0.013	0.09	0.058	4.445	1.097	0.865	0.867
a7	-4.794	0.849	-0.158	0.009	0.299	0.151	4.946	0.927	0.858	0.879
a8	-4.735	0.849	0.158	0.009	0.299	0.151	4.946	0.927	0.935	0.906
a9	-4.741	0.545	0.946	0.089	0.224	0.906	4.326	0.94	0.931	0.85
a10	-4.624	0.77	0.131	0.094	0.742	0.926	3.581	1.374	0.952	0.89
a11	-4.65	0.566	0.553	0.057	0.108	0.539	3.302	1.326	0.861	0.937
a12	-4.664	0.467	0.985	0.047	0.027	0.108	4.603	0.985	0.95	0.875
a13	-4.755	0.474	0.636	-0.045	0.935	0.998	4.295	1.12	0.935	0.873
a14	-4.767	-0.769	0.867	-0.04	0.995	0.99	5.668	1.19	0.859	0.895
a15	-4.779	0.339	0.871	-0.044	0.02	0.105	5.56	0.949	0.867	0.873
a16	-4.907	0.773	0.916	-0.112	0.848	0.991	5.08	1.037	0.907	0.8967
a17	-4.958	0.866	-0.706	-0.04	0.027	0.969	5.373	1.121	0.898	0.906
a18	-4.961	0.637	0.604	0.018	0.036	0.05	5.586	0.922	0.916	0.889
a19	-4.832	0.784	0.903	-0.316	0.999	0.859	6.005	0.898	0.859	0.91
a20	-4.877	0.854	0.24	-0.056	0.565	0.833	6.289	0.941	0.819	0.9
a21	-4.884	0.378	0.58	-0.121	0.973	0.05	6.359	0.782	0.851	0.881
a22	-4.839	0.007	0.444	0.931	0.062	0.097	4.643	1.583	0.923	0.931
a23	-4.927	0.08	0.016	0.001	0.011	0.044	4.318	1.524	0.866	0.939
a24	-4.922	0.009	0.683	0.03	0.004	0.095	4.855	1.337	0.899	0.924
a25	-4.705	0.03	0.652	-0.134	0.041	0.325	3.989	1.299	0.978	0.896
a26	-4.885	0.091	0.02	-0.009	0.47	0.023	4.003	1.221	0.995	0.891
a27	-4.854	0.109	0.951	-0.003	0.01	0.626	4.949	1.107	0.993	0.884
a28	-4.861	0.11	0.053	0.188	0.99	0.184	5.309	1.242	0.79	0.793
a29	-4.992	0.015	0.916	0.132	0.007	0.055	6.309	1.164	0.803	0.863
a30	4.941	0.026	0.085	-0.063	0.178	0.117	7.149	1.278	0.776	0.88
a31	-4.968	0.004	0.865	0.208	0.043	0.028	0.503	1.659	0.874	0.817
a32	-4.96	0.021	0.145	0.095	0.998	0.286	2.812	2.019	0.759	0.822
a33	4.856	0.01	0.302	0.195	0.008	0.051	4.577	1.541	0.933	0.958
a34	-4.834	0.004	0.421	0.115	0.002	0.019	4.028	1.788	0.943	0.944
a35	-4.27	0.015	0.789	-0.047	0.999	0.985	4.35	1.04	0.996	0.863
a36	-4.27	0.015	0.789	-0.047	0.999	0.985	4.35	1.04	0.996	0.863
a37	-4.77	0.015	0.789	-0.047	0.999	0.985	4.581	1.04	0.996	0.803
a38	-4.885	0.091	0.02	0.09	0.47	0.203	4.003	1.221	0.995	0.891
a39	-4.885	0.091	0.02	0.09	0.47	0.203	4.003	1.221	0.995	0.891
a40	-4.885	0.091	0.02	0.09	0.47	0.203	4.003	1.221	0.995	0.891
a41	-4.885	0.091	0.02	0.09	0.47	0.203	4.003	1.221	0.995	0.891
a42	-4.885	0.091	0.02	0.09	0.47	0.203	4.003	1.221	0.995	0.891
a43	-4.885	0.091	0.02	0.09	0.47	0.203	4.003	1.221	0.995	0.891
a44	-4.885	0.091	0.02	0.09	0.47	0.203	4.003	1.221	0.995	0.891
a45	-4.885	0.091	0.02	0.09	0.47	0.203	4.003	1.221	0.995	0.891
a46	-4.885	0.091	0.02	0.09	0.47	0.203	4.003	1.221	0.995	0.891

a47	-4.885	0.091	0.02	0.09	0.47	0.203	4.003	1.221	0.995	0.891
a48	-4.885	0.091	0.02	0.09	0.47	0.203	4.003	1.221	0.995	0.891
a49	-4.885	0.091	0.02	0.09	0.47	0.203	4.003	1.221	0.995	0.891
a50	-4.885	0.091	0.02	0.09	0.47	0.203	4.003	1.221	0.995	0.891

he ADMET evaluation of the designed pyrazolone derivatives (A1–A50) demonstrated variable pharmacokinetic and toxicity profiles. A few compounds, particularly A3, A22, A31, and A32, exhibited relatively better absorption, distribution, and metabolic stability compared to the rest of the series. These compounds showed acceptable permeability, moderate volume of distribution, and lower cytochrome P450 inhibition, indicating a more favorable drug-like profile.

4.4 DOCKING

From the docking result of 50 derivatives 25 derivatives which shows high and similar docking score than standard drug is shown in the table.

Table 4: binding affinity.

COMPOUND CODE	R GROUP	DOCKING SCORE
a1	C_6H_6	-5.70
a2	$C_6H_5OCH_3$	-6.15
a3	$C_6H_5OC_2H_5$	-6.32
a4	C_6H_5F	-5.32
a5	C_6H_5F	-6.75
a6	C_6H_5F	-5.06
a7	$C_6H_5OCH_3$	-5.29
a8	C_6H_5Cl	-6.78
a9	C_6H_5Cl	-5.32
a10	C_6H_5Br	-5.78
a11	C_6H_5Br	-5.44
a12	C_6H_5Br	-6.32
a13	C_6H_5Cl	-6.21
a14	$C_6H_5CH_3$	-5.28
a15	$C_6H_5OCH_3$	-5.28
a16	$C_6H_5OCH_3$	-5.05
a17	$C_6H_5OCH_3$	-6.13
a18	$C_6H_5OC_2H_5$	-5.84
a19	$C_6H_5OC_2H_5$	-5.68
a20	$C_6H_5OC_2H_5$	-5.88
a21	$C_6H_5OC_2H_5$	-5.58
a22	$C_6H_5NH_2$	-5.60
a23	$C_6H_5NH_2$	-5.17
a24	$C_6H_5NH_2$	-5.74

a25	$C_6H_5NO_2$	-5.33
a26	$C_6H_5NO_2$	-5.64
a27	$C_6H_5NO_2$	-5.61
a28	C_6H_5OH	-5.82
a29	C_6H_5OH	-5.82
a30	C_6H_5OH	-5.72
a31	$C_6H_5(OH)_2$	-5.48
a32	$C_6H_5(OH)_2$	-6.49
a33	$C_6H_5(NH_2)_2$	-5.11
a34	$C_6H_5(Cl)_3$	-5.24
a35	$C_6H_5(Cl)_3$	-5.65
a36	$C_6H_5(Cl)_2$	-5.28
a37	$C_6H_5(Cl)_2$	-6.07
a38	$C_6H_5(Cl)_2$	-5.50
a39	$C_6H_5(Cl)_2$	-5.25
a40	$C_6H_5(F)_2$	-4.93
a41	$C_6H_5(F)_2$	-4.93
a42	$C_6H_5(F)_2$	-5.54
a43	$C_6H_5(Br)_2$	-5.74
a44	$C_6H_5(Br)_2$	-5.59
a45	$C_6H_5(Br)_2$	-5.66
a46	$C_6H_5(Br)_2$	-5.38
a47	$C_6H_5(F)_2$	-4.98
a48	$C_6H_5(Cl)_2$	-6.25
a49	$C_6H_5(OH)_2$	-6.90
a50	$C_6H_5(CH_3)_2$	-5.25
STANDARD (Ritonavir)		-5.00

SUMMARY AND CONCLUSION

Summary

The present work deals with the synthesis of certain novel PYRAZOLONE derivatives and exploring their anti-viral. The investigation that has been carried out is summarized below under separate headings.

I. MOLINSPIRATION

All compounds (a1–a50) were evaluated using Lipinski's Rule of Five and showed zero violations, indicating excellent drug-likeness. Molecular weights were within acceptable limits (<500 Da), while hydrogen bond donors (0–4) and acceptors (6–9) supported good permeability.

Log P values (-0.31 to 3.09) reflected balanced lipophilicity, and rotatable bonds (3–5) indicated suitable molecular flexibility. Overall, these results suggest that all compounds possess favorable properties for oral bioavailability and are promising candidates for further studies.

II. PASS

All compounds exhibited Pa values higher than Pi, indicating a greater likelihood of biological activity. The Pa values ranged from 0.155 to 0.277, while Pi values remained comparatively lower, supporting the predicted activity of the compounds.

Notably, compounds such as a26 (Pa = 0.277), a28 (Pa = 0.273), and a32 (Pa = 0.268) demonstrated relatively higher Pa values, suggesting stronger potential biological activity. In contrast, compounds like a35–a37 showed lower Pa values, indicating comparatively weaker predicted activity.

Overall, the results suggest that most compounds possess moderate predicted biological activity, with several candidates showing promising potential for further pharmacological evaluation.

III. ADMET

Compound a3 exhibited the highest activity due to its excellent absorption profile, as indicated by the highest MDCK permeability, along with moderate P-glycoprotein inhibition that supports better bioavailability. It also shows a balanced distribution (VDss) and favorable metabolic behavior with minimal CYP inhibition, reducing the risk of drug–drug interactions. Furthermore, its clearance and half-life values indicate an optimal elimination rate, while low DILI and carcinogenicity values confirm an acceptable safety profile. Collectively, these properties make compound a3 the most promising candidate among the studied series.

IV. DOCKING STUDIES

Compound A49 exhibited the highest docking activity with a score of -6.90, which is significantly better than the standard (Ritonavir, -5.00), indicating a stronger binding affinity toward the target protein. This enhanced activity may be attributed to the presence of the dihydroxy (C6H5(OH)2) substituent, which can form strong hydrogen bonding interactions with the active site residues, thereby stabilizing the ligand–protein complex. Additionally, other compounds such as A8 (-6.78) and A5 (-6.75) also showed good binding affinity, likely

due to electronegative substituents like chlorine and fluorine that enhance hydrophobic and halogen interactions. Overall, compound A49 stands out as the most promising candidate based on docking results.

CONCLUSION

In this study, a systematic in silico approach was employed to design and evaluate novel pyrazolone derivatives derived from imidazole hydrazide as potential SARS-CoV-2 main protease inhibitors. Fifty compounds were successfully designed and screened for drug-likeness, all of which satisfied Lipinski's rule of five, indicating favorable oral bioavailability. PASS prediction and ADMET analysis suggested acceptable biological activity profiles and pharmacokinetic properties. Molecular docking studies against the SARS-CoV-2 Mpro (6LU7) revealed that several compounds exhibited strong binding affinities, comparable to or exceeding that of the reference drug ritonavir. Notably, compound A49 showed the highest docking score, highlighting its potential as a lead molecule. These findings suggest that pyrazolone-based scaffolds hold significant promise in antiviral drug discovery. Further synthesis, in vitro, and in vivo studies are warranted to validate the antiviral efficacy and therapeutic potential of the identified lead compounds.

REFERENCE

1. Duboc C, Flitsch SL. Drug discovery and development. *JACS Au*, 2024; 4(2): 276–278.
2. Rommasi F, Nasiri MJ, Mirsaeid M. Antiviral drugs proposed for COVID-19: mechanism and pharmacological data. *Eur Rev Med Pharmacol Sci*, 2021; 25: 4163–4173.
3. Guo C, Xu H, Li X, Yu J, Lin D. Suramin disturbs the association of the N-terminal domain of SARS-CoV-2 nucleocapsid protein with RNA. *Molecules*, 2023.
4. Liao ML, Liu PP, Tan CL, Li PG, Zou LH. Advances in pyrazolone functionalization: a review since 2020. *Tetrahedron*, 2026; 192: 135103.
5. Kwan EE, et al. ACD/Spectrus processor review. *J Chem Inf Model*, 2012; 52(7): 1898–1900.
6. Bernstein FC, Koetzle TF, et al. The Protein Data Bank: a computer-based archival file for macromolecular structures. *J Mol Biol*., 1977; 112(3): 535–542.
7. Berman HM, Battistuz T, Bhat TN, et al. The Protein Data Bank. *Acta Crystallogr D Biol Crystallogr*, 2002; 58(6): 899–907.
8. Berman HM, Westbrook J, Feng Z, et al. The Protein Data Bank. *Nucleic Acids Res*, 2000; 28(1): 235–242.

9. Kitchen DB, Decornez H, Furr JR, Bajorath J. Docking and scoring in virtual screening for drug discovery: methods and applications. *Nat Rev Drug Discov*, 2004; 3(11): 935–949.
10. Jakhar R, Dangi M, Khichi A, Chhillar AK. Relevance of molecular docking studies in drug designing. *Curr Bioinform*, 2020; 15(4): 270–278.
11. Goodsell DS, Morris GM, Olson AJ. Automated docking of flexible ligands: applications of AutoDock. *J Mol Recognit*, 1996; 9(1): 1–5.
12. Morris GM, Huey R, Olson AJ. Using AutoDock for ligand–receptor docking. *Curr Protoc Bioinformatics*, 2008; 24(1): 8–14.
13. Fernandes TB, Segretti MC, Polli MC, Parise-Filho R. Analysis of the applicability and use of Lipinski's rule for central nervous system drugs. *Lett Drug Des Discov*, 2016; 13(10): 999–1006.
14. Matta R, Pochampally J, et al. Design, synthesis and molecular docking studies of triazole–pyrazolone–thiazole derivatives as potential antimicrobial and anti-COVID-19 agents. *J Mol Struct*, 2022; 1250: 131824.
15. Batool S, et al. SARS-CoV-2 drug resistance and therapeutic approaches: a comprehensive review. *J Mol Struct*, 2022; 1247: 131304.